A survey of commercial soda–lime–silica glass compositions: Trends and opportunities. I—Compositions, properties and theoretical energy requirements

DENG, Wei, WAKELIN, Elliott, KILINC, Erhan and BINGHAM, Paul A. <http://orcid.org/0000-0001-6017-0798>

Received: 21 March 2024 | Revised: 28 August 2024 | Accepted: 16 September 2024

DOI: 10.1111/ijag.16691

INTERNATIONAL JOURNAL OF Applied Glass SCIENCE

RESEARCH ARTICLE

A survey of commercial soda–lime–silica glass compositions: Trends and opportunities. I—Compositions, properties and theoretical energy requirements

Wei Deng | **Elliott Wakelin** | **Erhan Kilinc** | **Paul A. Bingham**

Materials and Engineering Research Institute, Sheffield Hallam University, Sheffield, UK

Correspondence
Wei Deng and Paul A. Bingham, Materials and Engineering Research Institute, Sheffield Hallam University, Sheffield S1 1WB, UK.
Email: wei.deng@shu.ac.uk and p.a.bingham@shu.ac.uk

Funding information
UK Research and Innovation, Grant/Award Number: EP/V054627/1

Abstract

This research aimed to investigate the compositions of commercial soda–lime–silica glasses currently present in the UK market, as there is a lack of recent research on the subject, with the most recent studies now being over 20 years old. This study involved sampling and analyzing the compositions of over 30 commercial soda–lime–silica container and float glass samples, primarily from the UK market, in 2022 to 2023. Based on the results, the characteristics of these commercial glasses has been evaluated using multiple property models and analysis methods. In the first part, we illustrated the opportunities for glass manufacturers to modify or adjust their glass compositions to enable lower melting temperatures, thereby reducing energy demand and fuel carbon emissions. This can help the glass industry meet its net zero carbon emissions targets. It de-risks compositional modifications for a glass manufacturer by highlighting that other manufacturers have already successfully commercially implemented such changes.

KEYWORDS
commercial glass compositions, decarbonization, energy efficiency, melting temperatures

1 | INTRODUCTION

The manufacture of soda–lime–silica glass for commercial applications uses energy-intensive processes that generate substantial global CO_2 emissions.[1] The global commercial glass sector accounts for the emission of roughly 86 million metric tons of CO_2,[1,2] or about 0.3% of total worldwide CO_2 emissions, according to an International Energy Agency (IEA) report from 2020.[3] In the United Kingdom, the government has pledged to achieve the ambitious goal of achieving net-zero greenhouse gas emissions by the year 2050.[4] In our previously research,[5] an outlook of some potential routes to help the glass industry to achieve net-zero were discussed based on the current UK decarbonization policy. The forthcoming two to three decades will play a crucial role in initiating changes and achieving decarbonization before stable low-carbon energy carriers are adopted and firmly established.[5] As a result, there will be a transitional phase involving substantial alterations to current practices and materials in the glass industry, including raw materials for glass batch, compositions, production processes, fuels, and furnace

designs, in line with the anticipated implementation of the net-zero policy.[5] New melting designs/technologies and novel alternative batch compositions will continue to emerge and vary according to region.[5] Currently, we are witnessing the emergence of various explorations and studies in both academic and industrial domains, and these endeavors are progressing at a rapid pace, with interesting results. According to the Glass Decarbonization Roadmaps to 2050[6] and Glass sector Net zero strategy 2050,[4] 75%–85% glass industrial CO_2 emissions arise from the combustion of fuel and 15%–25% from the decomposition of carbonate raw materials. Fuel switching and alternative glass batches/compositional reformulation are highlighted among the most promising means of achieving decarbonization. Glass Futures, as a nonprofit organization in the UK, is guiding the development of new technologies, to help the UK and global glass industries decarbonize. Its new £54 m Global Centre of Excellence in St Helens, UK, which opened in June 2023, will be involved in studies of hydrogen fuels, low-cost biofuels and electrical boosting projects that could pave the way for the glass and ceramic industries to cut their carbon emissions.[7] In 2022, Glass Futures, along with one of its core members, Pilkington UK Ltd (a part of NSG Group) were involved in a £1.7 m BEIS (the department for Business, Energy, and Industrial Strategy)-funded project to demonstrate the feasibility of low-cost carbon capture solutions in hard-to-decarbonize industries such as glass.[8] In response to the call of alternative glass batch/reformulation, our research group[5,9–12] has delivered a series of studies on this topic, including an investigation on potential alternative resources for glass additives within the UK.[9] From 2017 to 2018, a research on the briquetting of waste glass cullet fine particles for energy-saving glass manufacture has been successfully applied to actual glass production.[11,12] From 2018 to 2022, a series of projects named as EnviroAsh (UKRI-funded), EnviroGlass 2 (UKRI-funded) and BiomAsh (BEIS-funded) have indicated that the utilization of biomass ash presents a promising prospect for introducing a novel raw material that could contribute significantly to advancing the decarbonization efforts within the glass industry.[5,10,13–15]

The development of new technologies is inspiring. However, it still needs to undergo the test of commercial practice. Most importantly, new technologies should play an active role in supporting the commercialization and sustainability aspects of achieving net-zero goals. Moreover, the pathways to achieving zero carbon emissions will vary across different regions due to specific resources, costs, and national conditions.

In view of this, our research has included focusing on the innovation of current commercial glass compositions.[5,9–12] However, it is first vital to have a clear understanding of current commercial glass compositions. Glass composition is a crucial aspect of commercial glass technology as it is closely related to all aspects of glass production processes. It directly relates to, and impacts upon, the sources and costs of raw materials, refractories, furnace design, production equipment, product quality requirements, as well as the production techniques. Correspondingly, compared to changes in other manufacturing processes, the adjustment of glass composition can, in many situations, be relatively low-cost and provide high flexibility. It can be said that driven by factors such as cost, product performance, and manufacturing processes, capacity to adjust glass composition contributes to the glass industry's flexibility in production and its ability to respond to the market demands. Commercial glass compositions are influenced by multiple factors, including cost, product performance, and manufacturing processes such as melting and forming. These factors are closely related to the level of technological advancement in the glass industry and within particular companies, and even at individual sites.

In this work, we have investigated the chemical compositions of thirty container glass samples and four float glass samples collected from the UK market between 2022 and 2023. Based on the results of the compositional analyses, The physical and chemical properties of these commercial glasses have been evaluated using multiple models. The composition differences we observed in current glasses suggest that with slight adjustments to the glass compositions used by some manufacturers, their furnace temperatures could significantly decrease, consequently reducing fuel consumption and CO_2 emissions. Moreover, the fact that other manufacturers are already successfully manufacturing glass with that composition, substantially de-risks any such changes to glass composition for a given glass manufacturer.

2 | EXPERIMENTAL PROCEDURES

2.1 | Sample collection

A total of 30 container glasses were gathered from UK supermarkets, comprising 10 amber, 10 green, and 10 colorless (flint) container glasses. Each sample was manufactured by a different company, and their place of production was identified via the registered trademark (punt mark) on the bottom of each container.[16] These have been anonymized for the purposes of this study. The glass sample numbers, and their identified places of origin, are listed in Table 1. Furthermore, four float glass samples were

TABLE 1 Commercial glass samples collected from the UK market.

Type	Sample	Country of origin	Type	Sample	Country of origin
Amber container	A01	UK	Flint container	F01	UK
	A02	UK		F02	UK
	A03	UK		F03	UK
	A04	UK		F04	UK
	A05	EU		F05	UK
	A06	UK		F06	UK
	A07	UK		F07	UK
	A08	USA		F08	UK
	A09	Ireland		F09	India
	A010	USA		F010	Denmark
Green container	G01	UK	Float	Float01	UK
	G02	UK			
	G03	UK		Float02	UK
	G04	UK			
	G05	EU		Float03	UK
	G06	Italy			
	G07	EU		Float04	Türkiye
	G08	Spain			
	G09	France			
	G010	UK			

TABLE 2 Estimated experimental normalized uncertainties for X-ray fluorescence (XRF) measurement (wt %).

SiO_2 (%)	Al_2O_3 (%)	Fe_2O_3 (%)	CaO (%)	MgO (%)	Na_2O (%)	K_2O (%)	TiO_2 (%)	ZrO_2 (%)	SO_3 (%)	Cr_2O_3 (%)	Sum (%)
.536	.029	.001	.049	.021	.148	.012	.001	.001	.019	.001	.560

obtained from different manufacturers and are also listed in Table 1.

2.2 | X-ray fluorescence (XRF) analyses

All glasses samples were sent to Glass Technology Services Ltd., for sample preparation and high-accuracy XRF quantitative compositional analysis using a fully-calibrated oxide XRF program specially designed for commercial soda–lime–silica glass compositional analysis. After being cut using a hot wire method,[17] glass samples were ground and polished using a diamond pad until the surface had a perfect mirror finish. XRF spectroscopy was employed to ascertain the chemical compositions (WDXRF, Bruker AXS—S4 PIONEER). A modified version of the OXI program was employed for the analysis of the XRF data.[5,18] Estimated experimental uncertainties for the soda lime silica (solid glass/container glass) calibration method are shown in Table 2. These were calculated using the Certified Reference Material SGT11 glass from the Society of Glass Technology.[19]

2.3 | Glass density measurement

Densities were determined using an electronic density meter (Mettler TOLEDO™ New Classic MS) based on the Archimedes principle:

$$\rho = \left[\frac{W_A}{W_A - W_W}\right] \delta_W$$

Here, ρ represents the density in g·cm^{-3}, W_A is the glass weight in air, W_W is the glass weight in water, and δ_W denotes the water density with temperature correction.

Before measurement, samples were cleansed with isopropanol to eliminate any debris and then immersed in distilled water at a known room temperature. The density of distilled water was corrected at the measured

temperature. The mean density of each glass was calculated by averaging five independent measurements.

2.4 | Liquidus temperature measurement

In order to validate the liquidus temperatures calculated based on the composition model, several samples were selected in this study for liquidus temperature measurement, and the results were compared with the calculated values to ensure their accuracy.

The liquidus point characterizes the maximum temperature allowing for the coexistence of the glass melt and the primary crystalline phase in equilibrium.[20] In order to validate the liquidus temperatures calculated based on the composition model, several samples were selected in this study for liquidus temperature measurement, and the results were compared with the calculated values to ensure their accuracy.

The gradient boat method was employed to measure the liquidus temperatures,[21] approximately 10 g of the glass sample were crushed in a stainless-steel mortar and then placed in boats made of either alumina (from Almath® BS91) or platinum (from Sigma Aldrich Z685429). The glass samples were held in the furnace for 24 hours within a known temperature gradient and then quenched in air to cool to room temperature. The liquidus temperatures of the glass samples were determined by observing the devitrification within the bulk glass using an Alicona Infinitefocus optical microscope.[21]

3 | GLASS PROPERTY MODELING

Utilizing the chemical compositions of glass samples, essential viscosity points, such as melting point, working point, softening point, and annealing point, were modeled employing both the Lakatos[22] and Fluegel[23] models, as outlined in Tables 3 and 4. Furthermore, the study involved the computation of the relative machine speed (RMS), working range index (WRI), and devitrification index (D)[1,9] for each glass formulation (refer to Tables 3 and 4). RMS is a commonly employed term in glass manufacturing, representing the relative average speed at which articles can be produced using a specific glass composition[24]:

$$\mathrm{RMS} = \frac{S - 450}{(S - A) + 80}$$

Here, S represents the Littleton softening point in degrees Celsius, defined as the temperature corresponding to $\log(\eta/\mathrm{dPa{\cdot}s}) = 7.65$, and A denotes the annealing point in degrees Celsius, defined as the temperature corresponding to $\log(\eta/\mathrm{dPa{\cdot}s}) = 13.0$, where η is the melt viscosity in dPa·s. The WRI is defined as the temperature difference between the softening point (S) and the annealing point (A). WRI serves as an indicator of the working range and should not be confused with the actual working range. For most commercial soda–lime–silica container glasses, WRI exceeds 160°C[1,25]:

$$\mathrm{WRI} = (S - A)$$

The utilization of the devitrification index (D) in previous studies aimed to gauge the potential occurrence of devitrification issues.[1,9,25] A positive D value signifies a state of reduced susceptibility to devitrification, while a negative value implies a growing probability of devitrification:

$$D = \mathrm{WRI} - 160°\mathrm{C}$$

Here, WRI represents the working range index, as previously defined. While values of D can differ, a consensus of +15°C had become widespread in the global container glass industry by 2010.[1] The chemical durability/hydrolytic class of glasses are modelled using.[26] The liquidus temperatures of glasses were also modelled using the Fluegel method.[27]

4 | RESULTS

4.1 | XRF

The XRF analyses for container glasses are presented in Table 3 and for float glasses in Table 4.

4.2 | Glass properties

The results of modeled glass properties are listed in Table 5 to 8.

5 | DISCUSSION

5.1 | Current commercial glass melting temperature comparison

The melting temperature of glass significantly influences the energy consumption and thermal efficiency of the furnace.[5] The energy efficiency of traditional flame furnaces is closely associated with carbon emissions, with a

TABLE 3 X-ray fluorescence (XRF) analyses of commercial container glasses.

Sample (wt%)	A01	A02	A03	A04	A05	A06	A07	A08	A09	A010
SiO_2	71.329	70.912	71.448	72.71	71.892	70.921	70.824	71.357	71.284	73.192
Al_2O_3	1.991	2.374	1.988	1.515	1.827	2.056	2.345	1.851	2.152	1.393
Fe_2O_3	.445	.536	.537	.35	.338	.629	.548	.419	.472	.481
CaO	11.048	10.243	10.774	10.177	10.6	10.951	10.284	10.529	10.731	11.182
MgO	1.194	2.077	1.355	1.259	1.608	1.468	2.117	2.058	2.238	0.316
Na_2O	13.038	12.757	13.199	13.378	13.091	13.198	12.799	12.752	12.151	13.034
K_2O	.754	.921	.493	.419	.477	.511	.889	.864	.798	.243
TiO_2	.081	.094	.112	.085	.080	.120	.100	.057	.07	.049
ZrO_2	.010	.008	.014	.013	.009	.017	.009	.014	.014	.004
SO_3	.068	.059	.052	.061	.045	.089	.066	.044	.051	.093
Cr_2O_3	.042	.019	.028	.033	.033	.040	.019	.055	.039	.013
Sum	100.000	100.000	100.000	100.000	100.000	100.000	100.000	100.000	100.000	100.000
Sample (wt%)	**F01**	**F02**	**F03**	**F04**	**F05**	**F06**	**F07**	**F08**	**F09**	**F010**
SiO_2	71.945	72.693	71.977	72.597	72.654	72.738	72.552	72.459	70.378	72.707
Al_2O_3	1.229	1.686	1.741	1.372	1.241	1.209	1.725	1.533	1.531	1.215
Fe_2O_3	.070	.058	.068	.059	.067	.077	.057	.027	.129	.057
CaO	11.095	11.079	11.571	11.609	11.715	11.258	11.153	9.901	10.244	11.767
MgO	1.968	.676	.762	1.688	1.708	1.876	.71	2.258	2.802	1.695
Na_2O	13.106	13.088	13.118	12.055	12.026	12.224	13.052	13.524	14.071	11.961
K_2O	.383	.522	.575	.404	.398	.391	.561	.04	.523	.346
TiO_2	.057	.056	.055	.059	.05	.049	.053	.044	.072	.036
ZrO_2	.004	.004	.004	.004	.005	.004	.004	.003	.010	.008
SO_3	.141	.136	.126	.151	.133	.172	.132	.210	.239	.206
Cr_2O_3	.002	.002	.003	.002	.003	.002	.001	.001	.001	.002
Sum	100.000	100.000	100.000	100.000	100.000	100.000	100.000	100.000	100.000	100.000
Sample (wt%)	**G01**	**G02**	**G03**	**G04**	**G05**	**G06**	**G07**	**G08**	**G09**	**G010**
SiO_2	71.105	70.375	71.355	71.176	70.936	71.556	72.306	71.329	71.992	69.846
Al_2O_3	1.835	1.831	1.583	1.772	2.299	1.568	1.302	2.045	1.541	1.769
Fe_2O_3	.501	.481	.356	.216	.538	.540	.420	.313	.321	.215
CaO	10.928	10.884	11.479	11.674	10.759	10.656	11.148	10.452	10.957	10.030
MgO	2.205	2.027	1.021	1.200	1.377	1.767	1.413	2.012	1.214	3.006
Na_2O	12.318	13.267	13.246	13.196	12.736	12.947	12.626	12.691	13.115	14.372
K_2O	.728	.741	.592	.570	1.022	.629	.445	.866	.569	.343
TiO_2	.068	.067	.063	.082	.057	.049	.050	.055	.052	.062
ZrO_2	.010	.012	.008	.011	.010	.007	.007	.011	.011	.004
SO_3	.080	.102	.059	.031	.043	.065	.068	.027	.021	.120
Cr_2O_3	.222	.213	.238	.072	.223	.216	.215	.199	.207	.233
Sum	100.000	100.000	100.000	100.000	100.000	100.000	100.000	100.000	100.000	100.000

[†]Amber (labeled as A*); Flint (F*); Green (G*).

study indicating that 75%–85% glass industrial CO_2 emissions arise from the combustion of fuel.[4] Generally, people tend to focus on the quantity of heat losses, which is crucial when evaluating the furnace's performance in terms of energy consumption.[28,29] Although the operating temperature (hot spot temperature) of commercial glass furnaces is widely believed to fall within the range of 1450 to 1600°C,[1,30,31] there is limited discussion and research on the combined examination of glass composition, melting temperature, and their impact on energy consumption and carbon emissions. There are three main reasons for this. First, due to a lack of research, it is generally believed that the composition of ordinary commercial glass has changed little since 1990 as we discussed earlier. Second,

TABLE 4 X-ray fluorescence (XRF) analyses of commercial float glasses.

Sample (wt%)	Float01	Float02	Float 03	Float 04
SiO_2 (%)	72.279	72.394	71.776	72.137
Al_2O_3 (%)	.800	.626	1.130	.337
Fe_2O_3 (%)	.061	.062	.066	.054
CaO (%)	8.780	10.192	8.688	9.729
MgO (%)	4.016	3.011	4.231	3.420
Na_2O (%)	13.723	13.249	13.475	13.934
K_2O (%)	.110	.209	.368	.125
TiO_2 (%)	.025	.039	.048	.031
ZrO_2 (%)	<l.d	<l.d	<l.d	<l.d
SO_3 (%)	.205	.217	.217	.232
Cr_2O_3 (%)	.001	.001	.001	.001
Sum	100.000	100.000	100.000	100.000

the sizes of various furnaces, furnace designs, refractory materials, fuels, thermal processes, and operating systems vary. Third, in-depth discussions on related issues would require extensive and costly thermal calibration or simulation of different furnaces. Moreover, empirical estimates lack data and theoretical evidence and are not widely representative. Therefore, engaging in relevant discussions is relatively challenging.

Undoubtedly, reducing the theoretical glass melting temperature can decrease the operating temperature of glass furnaces. Figure 1 illustrates a significant variation in the temperature corresponding to log (η/dPa/s) = 2, considered equivalent to the melting temperature, among currently operational commercial container and float glass compositions. This variation is up to 33°C for the UK glass compositions. This indicates that some manufacturers are already using glass compositions with lower viscosities (melting temperatures) in actual production than others. Glass production enterprises should mutually consider taking advantage of such temperature differences, as this can lead to short-term energy savings and carbon reduction effects with minimal operational risk. Therefore, based on available data, we provide a rough estimate of how the differences in glass viscosities (melting temperatures) impact upon the theoretical energy consumption during glass melting.

5.2 | Theoretical energy requirement for glass melting

To clarify the impact of the melting temperature on energy consumption, considering that the energy used in glass melting constitutes 72.2% of the total energy consumption in container glass production,[31] in this section, we have applied Madivate's method to calculate the theoretical energy requirement (TER)[32] for all surveyed glass samples. Two green container glasses have been used as illustrative examples in the Supporting Information A. In the absence of confirmed information on the raw materials and their proportions used for the manufacture of each investigated glass, a set of glass raw material compositions commonly employed in industrial practice[1] (see Supporting Information B Table SB1) were utilized to design the raw material composition for green glass, as detailed in Table B2 of Supporting Information B.

However, this classic approach is problematic as there is an issue with $\Delta H_{glass}(T)$ term. According to the 2002 research of Kim and Matyáš,[33] there are discrepancies between the data from two references, Madivate (1998)[32] and Madivate et al. (1996),[34] where the values of b_i used for $\Delta H_{glass}(T)$ in Madivate (1998)[32] are not consistent. Kim and Matyáš provided the b_i values back-calculated from the f_i values given in the table 6 from the paper of Madivate et al. (1996).[34] However, according to our calculations, those modified parameters are still not suitable for application in our present study. Kim and Matyáš[33] also noted that their retroactive calculations may have had limited accuracies due to the study of only six glass samples, but apart from this, the Madivate method (1998)[32] could be applied.

In the present scenario, we have utilized the partial molar heat capacity coefficients of oxides in silicate glasses from Richet (1987)[35] and employed a modified four-term Maier-Kelley formula as below:

$$\bar{C}_{Pi} = a_i + b_i T + \frac{c_i}{T^2} + \frac{d_i}{T^{\frac{1}{2}}}$$

and

$$C_{Pg} = \sum_i x_i \bar{C}_{Pi}$$

to calculate and integrate the heat capacity of glasses with different compositions from room temperature (300 K) to the glass transition temperature (assumed to be 550°C or 823 K).

Simultaneously, we have employed the fitted parameters for silicate liquid heat capacities and equation from Stebbins et al. (1984)[36]:

$$C_{P\ liquid} = \sum_i x_i \bar{C}_{Pi}$$

to calculate and integrate the heat capacities of glasses with different compositions from the glass transition temperature (assumed to be 550°C) to the melting temperature (the temperature corresponding to log (η/dPa/s) = 2).

TABLE 5 Modeled glass properties of amber container glasses based on composition.

		A01	A02	A03	A04	A05	A06	A07	A08	A09	A010
Lakatos model viscosity in log (dPa/s)	2	1449.4	1465.8	1452.1	1463.9	1459.8	1444.8	1463.3	1458.7	1470.5	1459.3
	3	1180.7	1193.5	1181.6	1187.3	1188.1	1176.9	1191.6	1189.1	1201.8	1186.6
	4	1028.3	1038.6	1029	1032.8	1034.3	1025.6	1037.3	1035.5	1045.8	1032
	7.6	740.1	743.6	739.4	738.2	742.3	738.5	743.1	743.5	752.3	742.3
	13	563.2	565.7	562.9	559.4	564	563.1	565.5	564.5	570.9	562.1
WRI		176.8	177.9	176.5	178.8	178.3	175.4	177.5	178.9	181.4	180.3
RMS		1.129	1.138	1.128	1.114	1.131	1.13	1.138	1.133	1.157	1.123
D		16.8	17.9	16.5	18.8	18.3	15.4	17.5	18.9	21.4	20.3
Fluegel model Viscosity in log (dPa/s)	2	1449.3	1457.9	1451.7	1458.7	1455.7	1446.3	1455.9	1453.5	1463	1461
	2.5	1304.7	1312.4	1306.6	1312.7	1310.5	1301.9	1310.7	1308.8	1318.3	1315.6
	3	1191.9	1198.7	1193.4	1198.5	1197	1189.3	1197.2	1195.6	1204.9	1201.9
	4	1027.2	1032.3	1028	1031.4	1031.2	1025	1031.1	1030	1038.8	1035.8
	5	912.8	916.4	913.1	915.1	915.7	910.8	915.4	914.7	922.9	920.2
	7	764.2	765.5	763.9	763.7	765.5	762.7	764.9	764.6	771.9	769.8
	7.6	732.3	733.1	731.9	731.2	733.2	730.9	732.5	732.3	739.3	737.5
	9	671.9	671.6	671.3	669.6	672.1	670.7	671.2	671.2	677.7	676.4
	11	609.1	607.6	608.1	605.3	608.4	608	607.3	607.5	613.5	612.7
	11.5	596.3	594.6	595.4	592.4	595.6	595.4	594.4	594.6	600.5	599.8
	13	563.5	561.1	562.3	558.7	562.2	562.6	560.9	561.2	566.8	566.4
	13.3	557.7	555.2	556.5	552.8	556.4	556.8	555.1	555.3	560.9	560.6
WRI		168.8	172	169.5	172.4	171	168.3	171.5	171.1	172.5	171.1
RMS		1.134	1.123	1.13	1.114	1.128	1.131	1.123	1.124	1.146	1.145
D		8.8	12	9.5	12.4	11	8.3	11.5	11.1	12.5	11.1
Density (g/cm^3)		2.5143	2.5117	2.5134	2.5007	2.5077	2.5183	2.5127	2.511	2.5122	2.5038
Hydrolytic class		3	3	3	3	3	3	3	3	3	3
.01 M HCl to neutralize extracted basic oxides, (mL)		.62	.54	.61	.68	.59	.63	.55	.58	.49	.66
Cal. Liquidus T (°C)		1059	1058	1052	1024	1048	1061	1059	1056	1069	1034
ΔT_{FL} (T_{Log4} from Lakatos)		−30.7	−19.4	−23	8.8	−13.7	−35.4	−21.7	−20.5	−23.2	−2
ΔT_{FL} (T_{Log4} from Fluegel)		−31.8	−25.7	−24	7.4	−16.8	−36	−27.9	−26	−30.2	1.8
Exp. Liquidus T (°C)		1066	/	1056	/	/	1067	/	/	1073	/

Finally, the sum of these two integrations yields the enthalpy change from room temperature to the melting temperature, representing the $\Delta H_{glass}(T)$ term.

The calculated results for all glasses are presented in Table 9 and the melting temperatures (temperatures corresponding to $\log(\eta/\mathrm{dPa/s}) = 2$) have been calculated using the Fluegel model.[29]

According to the theory of Madivate,[32] the terms in Table 5 to 8 are explained as follows: ΔH_d represents the energy necessary to decompose the raw materials to their respective oxides; ΔH_g represents the energy involved in the formation, from the oxides, of the vitreous phases that are "existent" in the glass; ΔH_{glass} represents the heat required to heat the glass from room temperature to the melting temperature, this can also be interpreted as the heat necessary to melt a batch of 100% cullet glass; and ΔH_{gas} represents the heat required to heat the gas from room temperature to the glass melting temperature. The total energy requirement (TER) can be calculated by:

$$\mathrm{TER}\,(T)\left(\frac{\mathrm{kJ}}{\mathrm{kg\ of\ glass}}\right) = \Delta H_d + \Delta H_g + \Delta H_{glass} + b\Delta H_{gas}$$

where b represents the weight amount of gas ($1 + b$ kg of glass batch), CO_2 and H_2O are liberated during reaction of the batch.

TABLE 6 Modeled glass properties of flint container glasses based on composition.

		F01	F02	F03	F04	F05	F06	F07	F08	F09	F010
Lakatos viscosity in log (dPa/s)	2	1444.5	1460.8	1446.8	1464.5	1461.9	1464.8	1459.4	1465.9	1426.9	1462.4
	3	1179.3	1188.4	1179.8	1199.9	1198.5	1198.5	1187.9	1190.6	1160.9	1199.3
	4	1028.3	1033.9	1027.7	1044.5	1043.5	1043.3	1033.6	1036.5	1014.3	1044.1
	7.6	742.4	742.9	741.9	756.4	756.6	753.9	743.2	740.7	728.5	757.4
	13	563.7	563.5	564.2	572.1	572	569.7	563.9	562.3	556.7	572.4
WRI		178.7	179.4	177.7	184.3	184.6	184.1	179.3	178.3	171.8	184.9
RMS		1.13	1.129	1.133	1.159	1.159	1.15	1.131	1.125	1.106	1.16
D		18.7	19.4	17.7	24.3	24.6	24.1	19.3	18.3	11.8	24.9
Fluegel viscosity in log (dPa/s)	2	1443.4	1457.4	1447.6	1461.5	1460.2	1460.5	1456.4	1455.6	1424.9	1460.6
	2.5	1300.7	1312.6	1304.1	1318.0	1316.8	1316.9	1311.7	1311.5	1283.2	1317.6
	3	1189.0	1199.4	1192.1	1205.6	1204.6	1204.4	1198.6	1198.4	1172.4	1205.6
	4	1025.6	1033.8	1028.5	1040.8	1040.1	1039.4	1033.3	1032.6	1010.5	1041.3
	5	911.8	918.6	914.7	925.9	925.3	924.1	918.3	916.3	897.7	926.5
	7	763.6	768.7	766.9	776.1	775.8	773.8	768.7	764.8	751.1	776.9
	7.6	731.7	736.5	735.1	743.8	743.6	741.4	736.5	732.1	719.6	744.7
	9	671.4	675.5	675.1	682.7	682.6	680.0	675.6	670.2	659.9	683.6
	11	608.5	611.9	612.5	618.9	619.0	616.0	612.2	605.6	597.7	619.9
	11.5	595.8	599.1	599.8	606.0	606.1	603.0	599.4	592.5	585.2	607.0
	13	562.8	565.8	567.1	572.6	572.7	569.4	566.1	558.6	552.6	573.6
	13.3	557.0	559.9	561.3	566.7	566.9	563.5	560.3	552.6	546.9	567.7
WRI		168.9	170.7	168.1	171.2	170.8	172	170.3	173.6	167	171.1
RMS		1.132	1.143	1.15	1.17	1.17	1.156	1.144	1.113	1.092	1.174
D		8.9	10.7	8.1	11.2	10.8	12	10.3	13.6	7	11.1
Density (g/cm^3)		2.5055	2.5029	2.5109	2.5081	2.5088	2.5056	2.5041	2.4999	2.5162	2.5085
Hydrolytic class		3	3	3	3	3	3	3	3	4	3
.01 M HCl to neutralize extracted basic oxides, (mL)		.69	.67	.66	.56	.55	.6	.66	.72	.86	.59
ΔT_{FL} (T_{Log4} from Lakatos)		−27.7	−9.1	−31.3	−22.5	−24.5	−14.7	−12.4	7.5	−36.7	−23.9
ΔT_{FL} (T_{Log4} from Fluegel)		−30.4	−9.2	−30.5	−26.2	−27.9	−18.6	−12.7	3.4	−40.5	−26.7
Cal. Liquidus T (°C)		1056	1043	1059	1067	1068	1058	1046	1029	1051	1068
Exp. Liquidus T (°C)		1054	1048	1064	1079	/	/	1050	/	/	/

Based on the results shown in Table 5 to 8, the ΔH_{glass} and TER at the temperature corresponding to a viscosity of Log (η/dPa/s) = 2 for all current green, amber, flint and float glasses, are plotted in Figures 2 and 3 separately.

In Figure 2, different symbols and colors are used to distinguish between different container glasses and float glasses. Due to significant compositional differences, the ΔH_{glass} of float glass is higher than that of container glass. As the glass melting temperature varies between 1420°C and 1470°C, the ΔH_{glass} roughly ranges from 1820 kJ/kg to 1860 kJ/kg. The ΔH_{glass} of glass compositions within the investigated range generally increases with the rise in melting temperature, exhibiting a rough linear correlation between the two. This indicates that both the melting temperature and ΔH_{glass}, especially the former, collectively have an impact on the melting enthalpy.

The melting enthalpy ΔH_{glass} of glass compositions with melting temperatures below 1442°C in the surveyed samples increases relatively slowly with rising temperature. Taking G10 as an example, although its melting temperature is the lowest among the green glasses, its melting enthalpy is comparable to that of G03. However, when the melting temperature exceeds 1442°C, particularly in the range of 1445°C–1460°C among the surveyed glasses, the distribution of melting enthalpy undergoes more significant variations. Overall, there is obvious correlation

TABLE 7 Modeled glass properties of green container glasses based on composition.

		G01	G02	G03	G04	G05	G06	G07	G08	G09	G010
Lakatos viscosity in log (dPa/s)	2	1456.1	1433.2	1433.3	1435.3	1456.8	1450	1453.6	1463.7	1449.5	1422.8
	3	1190.5	1168.7	1168.7	1172.2	1186.5	1181.1	1186.2	1192.8	1180.1	1156.5
	4	1037	1019.8	1019.2	1022.3	1032.8	1029	1033	1038.3	1027.9	1010.9
	7.6	747.9	735.1	736.6	739.9	741.4	739.8	745.3	744.6	739.6	725.1
	13	567.9	560.9	560.8	564.1	564.2	561.6	564.4	565.6	561.5	555.8
WRI		180.1	174.3	175.8	175.9	177.3	178.1	180.9	179.1	178.1	169.3
RMS		1.146	1.121	1.12	1.133	1.133	1.123	1.132	1.137	1.122	1.103
D		20.1	14.3	15.8	15.9	17.3	18.1	20.9	19.1	18.1	9.3
Fluegel viscosity in log (dPa/s)	2	1455.1	1436.7	1440.8	1440	1455.4	1450.8	1456.1	1458	1451.1	1424
	2.5	1311.1	1293.6	1297.4	1296.9	1310	1306.2	1311.6	1312.9	1306.4	1281.8
	3	1198.5	1181.9	1185.6	1185.4	1196.5	1193.2	1198.7	1199.4	1193.4	1170.7
	4	1033.5	1018.8	1022.5	1022.7	1030.8	1028	1033.5	1033.2	1028.3	1008.5
	5	918.5	905.5	909.2	909.8	915.5	912.9	918.4	917.4	913.5	895.7
	7	768.7	758.3	762.2	763.3	765.7	763.3	768.6	766.6	764.3	749.2
	7.6	736.5	726.6	730.7	731.9	733.5	731.1	736.4	734.2	732.2	717.7
	9	675.5	666.9	671	672.5	672.6	670.2	675.5	672.8	671.6	658.1
	11	611.8	604.6	608.8	610.6	609.2	606.8	611.9	608.8	608.4	596.1
	11.5	599	592	596.3	598.1	596.4	593.9	599.1	595.8	595.6	583.5
	13	565.6	559.4	563.8	565.8	563.2	560.7	565.8	562.3	562.6	551.1
	13.3	559.8	553.7	558.1	560.1	557.3	554.9	560	556.4	556.8	545.4
WRI		170.9	167.3	166.9	166.2	170.3	170.4	170.6	171.9	169.7	166.6
RMS		1.142	1.119	1.137	1.145	1.133	1.123	1.143	1.128	1.13	1.085
D		10.9	7.3	6.9	6.2	10.3	10.4	10.6	11.9	9.7	6.6
density (g/cm^3)		2.5172	2.5222	2.5187	2.519	2.5152	2.5131	2.5109	2.5102	2.5104	2.5203
ΔT_{FL} (T_{Log4} from Lakatos)		−33	−46.2	−40.8	−47.7	−28.2	−21	−19	−18.7	−20.1	−41.1
ΔT_{FL} (T_{Log4} from Fluegel)		−36.5	−47.2	−37.5	−47.3	−30.2	−22	−18.5	−23.8	−19.7	−43.5
Cal. Liquidus T (°C)		1070	1066	1060	1070	1061	1050	1052	1057	1048	1052
Exp. Liquidus T (°C)		1057	1054	1047	1054	/	/	/	/	/	/

between the melting enthalpy of glass and changes in melting temperature.

Without knowledge of the glass batch composition in each case—which clearly has a significant impact on TER, we designed uniform batch rules for each type of glass based on practical considerations practical considerations, comparisons, and various other factors. In the current float glass practice in the UK, approximately 30% of cullet is typically added.[37] However, aiming to establish a standard without cullet, the design of this study incorporates 0% cullet in the batch for float glass. For flint glass packaging production, only flint glass cullet can be used, while for the production of green or amber glass, mixed-color cullet can be utilized. The higher the purity of cullet (same color), the larger the proportion that can be used for production.[38] The proportion of cullet in glass mixes can even exceed 90%, typically over 80% for green glass, around 60% for amber, and approximately 45%–50% for flint.[38] Considering the actual cullet usage in container glass production in the UK, along with balancing the glass composition within the scope of the survey, we set the cullet addition for flint glass batch at 56%. Moreover, to enhance the sample size for assessing the impact of melting temperature on TER, we set the cullet addition for green and amber glass batches at 66%. As shown in the Supplemental Information, the design of glass batch composition ensures consistency while preserving the necessary components, ensuring some level of comparability in the calculation of TER.

Due to space limitations, all information are condensed and presented in Figure 3. In the context of clarifying the relationship between TER, melting temperature, and cullet content, no further adjustments are made to the cullet content calculation. As depicted in Figure 3, and as

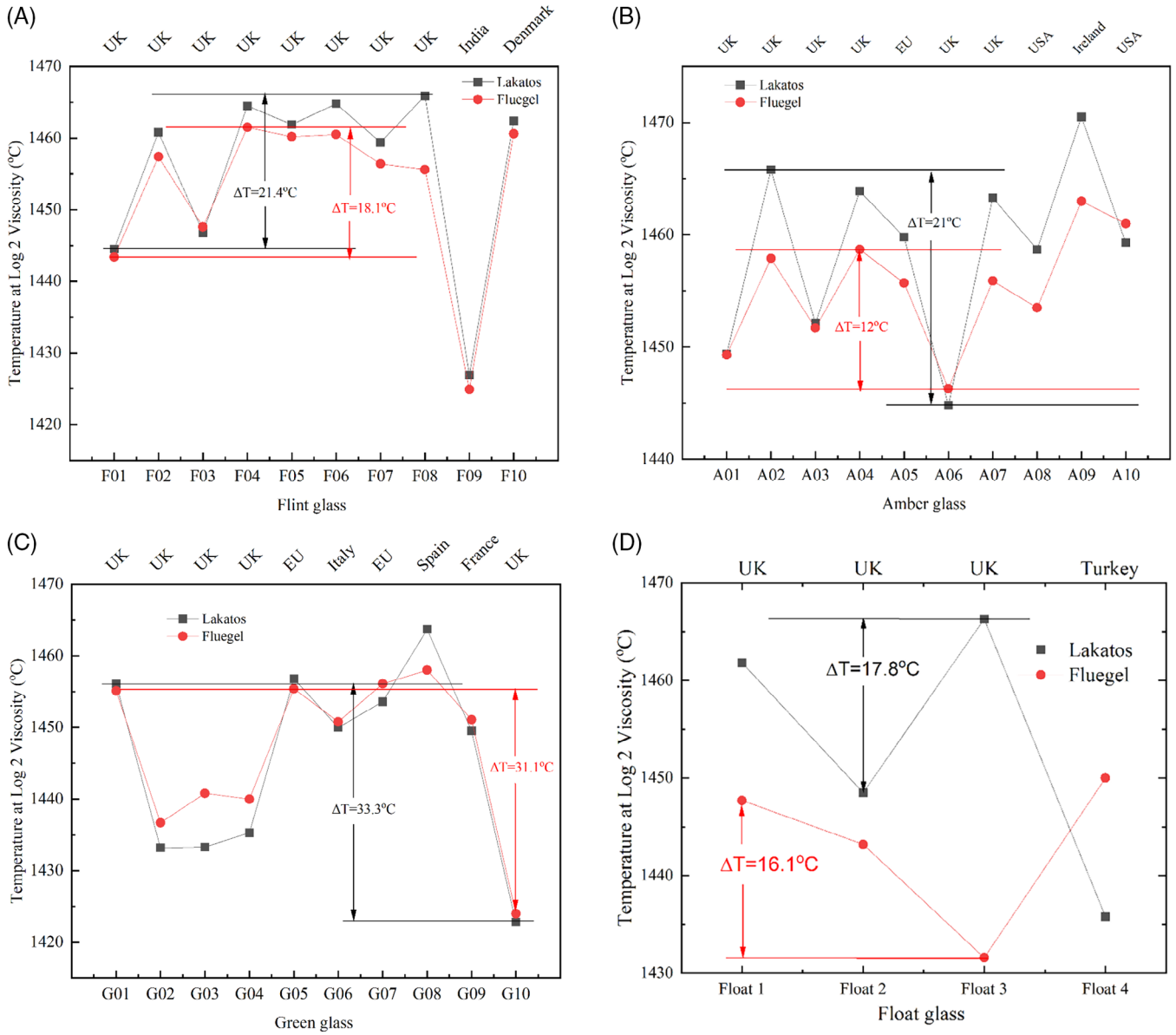

FIGURE 1 (A) Modeled flint container glasses at temperatures corresponding to log (η/dPa/s) = 2. (B) Modeled amber container glasses at temperatures corresponding to log (η/dPa/s) = 2. (C) Modeled green container glasses at temperatures corresponding to log (η/dPa/s) = 2. (D) Modeled float glasses at temperatures corresponding to log (η/dPa/s) = 2. The highest and lowest melting point difference as indicated in the diagram represents the melting point difference of glass in the United Kingdom.

is already known,[1] the content of cullet in the batch has a significant impact on TER. Float glass without cullet exhibits TER ranging from 2400 kJ/kg to 2450 kJ/kg; flint glass has TER in the range of 2025 kJ/kg to 2075 kJ/kg, while green and amber glasses have TER varying from 1975 kJ/kg to 2025 kJ/kg. Combining with Table 9, even though ΔH_{glass} accounts for 75%–92% of TER, when comparing glasses of the same type, TER exhibits a horizontal fluctuation with changing temperatures, unlike the trend in melting enthalpy. For example, in flint glass, F09 with the lowest melting temperature has TER only surpassed by F08; whereas in green glass, G010 with the lowest melting temperature has the highest TER. Observing Table 9, for glasses with reduced melting points achieved by increasing alkali metal content, such as F09 and F10, the energy required for raw material decomposition (ΔH_d) rises due to an increase in carbonate content, as calculated by the Madivate method.[32] This increase in energy is higher than the decrease in energy required for glass melting. Therefore, overall, under the same batch conditions, there is not necessarily a correlation between glass TER and melting temperature changes. However, this highlights the urgency of increasing the content of cullet in batch materials and finding alternative batch materials with lower

TABLE 8 Modeled glass properties of float glasses based on composition.

		Float 01	Float 02	Float 03	Float 04
Lakatos viscosity in log (dPa/s)	2	1461.8	1448.5	1466.3	1435.8
	3	1186.5	1180.8	1190.9	1167.7
	4	1034.4	1030	1038.1	1019.8
	7.6	736.3	740.5	738.4	731.5
	13	557.6	560.5	559.5	554.5
Fluegel viscosity in log (dPa/s)	2	1447.7	1443.2	1431.6	1450
	2.5	1305.3	1301	1290.2	1307.5
	3	1193	1189.4	1179.2	1195.1
	5	911	910.6	902	912.6
	7	758.3	760.7	752.9	759.6
	7.6	725.3	728.4	720.8	726.5
	9	662.5	667.1	659.8	663.6
	11	596.9	603.1	596.1	597.8
	11.5	583.6	590.1	583.2	584.5
	13	549.1	556.5	549.8	549.9
	13.3	543	550.6	544	543.8
Density (g/cm^2)		2.496	2.504	2.498	2.504
Hydrolytic class		3	3	3	4
Liquidus T (°C)		1008	1034	1016	1021

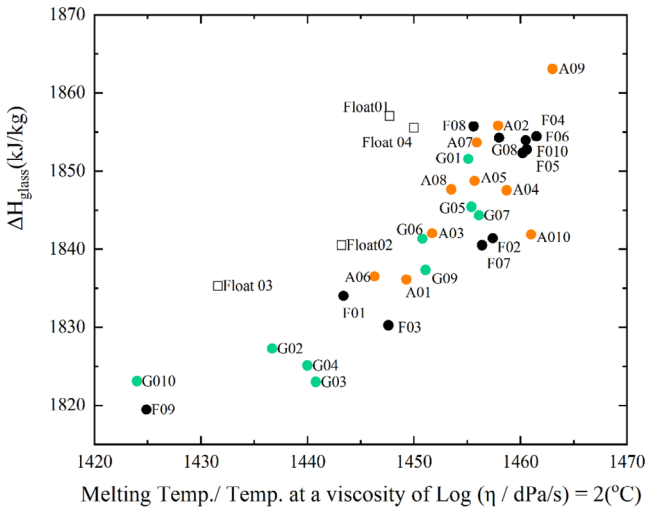

FIGURE 2 The ΔH_{glass} of all current glasses vs. temperature at a viscosity of log (η/dPa/s) = 2 for all current glasses.

decomposition energies, combined with compositional reformulation to reduce viscosities and hence furnace temperatures, fuel consumption, and CO_2 emissions.

5.3 | Operation temperature and furnace surface heat dissipation loss

The impact of log (η/dPa/s) = 2 (or melting, hot point/operation) temperature on the furnace surface heat

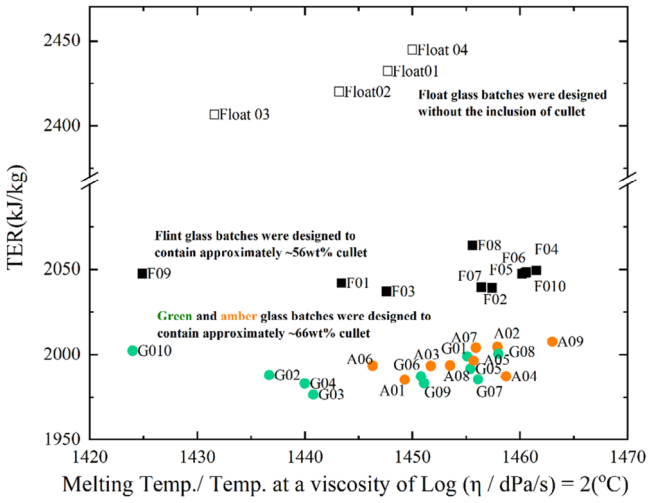

FIGURE 3 The theoretical energy requirement (TER) of all current n glasses vs. temperature at a viscosity of Log (η/dPa/s) = 2 for all current glasses.

losses by radiation in the atmosphere from the hot linings, which represent a major part of the energy consumption of glass melting furnaces,[31] is also noteworthy in studies related to carbon emission reduction and energy saving. However, this aspect was not reflected in the TER calculations in the previous section.

Taking a heat balance chart for a 39.7% thermal efficiency medium-sized melting tank in Japan in the 1990s as an example,[31] about 19.8% of the heat input is lost from wall of melting tank, 5.1% is lost from regenerator, and 17.9% lost form exhaust gas, flue and exchanger.[31] The total heat dissipation loss from furnace take 42.8% of heat input. And only 25.8% of the heat input is attributed to the heat carried out by glass and the reaction heat of the batch, therefore, the results of the TER calculations highlight certain issues but are not comprehensive. Specifically, the reduction in operating temperatures does not reflect the decrease in overall heat dissipation in the entire furnace in the TER.

In a model based on research published by Vishal et al.[29] in 2006, the heat loss from superstructure, furnace and walls was 9.2%, with 4.9% from the regenerator walls. As a complex system, the operational furnace temperature has a direct impact on the heat losses in the melting and heat exchange sections. However, there is a scarcity of reported studies on the relationship between the two.

The crown is the largest area of the furnace, where the heat losses are usually high at 1800–2000 W/m^2 or more.[39] We use it here as an example to provide an estimate of how the glass melting temperature (hence furnace temperature) affects heat loss from the crown. The heat transfer from furnace refractory walls is estimated based

TABLE 9 Theoretical energy requirement (TER) results for all glasses.

Country	Samples	ΔH_d (kJ/kg)	ΔH_g (kJ/kg)	ΔH_{glass} (kJ/kg)	ΔH_{gas} (kJ/kg)	TER (kJ/kg)
UK	Float01	1039.90	−506.31	1857.07	264.27	2432.19
UK	Float02	1051.68	−519.29	1840.52	279.55	2420.08
UK	Float03	1027.44	−495.15	1835.32	255.64	2406.77
Turkey	Float04	1075.55	−534.09	1855.51	281.92	2444.75
UK	F01	427.77	−229.25	1834.03	133.82	2042.16
UK	F02	416.06	−228.52	1841.38	138.95	2039.22
UK	F03	435.08	−239.46	1830.25	144.22	2037.11
UK	F04	386.87	−200.85	1854.43	130.37	2049.41
UK	F05	389.62	−203.7	1852.32	132.11	2047.47
UK	F06	386.28	−200.55	1853.93	127.25	2048.17
UK	F07	417.18	−228.53	1840.49	139.09	2039.47
UK	F08	415.03	−214.14	1855.72	119.65	2064.1
India	F09	461.69	−242.03	1819.43	125.69	2047.63
Denmark	F10	387.99	−201.48	1852.75	131.17	2048.34
UK	G01	293.57	−151.64	1851.55	101.56	1998.76
UK	G02	340.54	−186.61	1827.26	111.74	1987.77
UK	G03	347.88	−202.98	1823	126.47	1976.44
UK	G04	350.72	−201.4	1825.12	125.76	1982.89
EU	G05	304.05	−163.76	1845.42	107.05	1991.62
Italy	G06	312.64	−173.07	1841.33	109.1	1987.08
EU	G07	307.57	−173.3	1844.31	114.75	1985.43
Spain	G08	295.21	−154.16	1854.24	99.87	2000.37
France	G09	325.65	−187.26	1837.34	118.08	1983.04
UK	G010	376.95	−203.83	1823.09	106.61	2002.22
UK	A01	323.68	−181.5	1836.1	115.49	1985.26
UK	A02	292.48	−148.5	1855.8	95.53	2004.41
UK	A03	325.79	−181.37	1842.03	113.44	1993.16
UK	A04	311.41	−178.12	1847.54	110.3	1987.11
EU	A05	314.35	−172.93	1848.73	109.04	1996.29
UK	A06	334.55	−184.63	1836.49	114.27	1993.25
UK	A07	296.72	−151.14	1853.68	96.37	2003.98
USA	A08	299.43	−158.89	1847.64	101.86	1993.5
Ireland	A09	277.04	−137.11	1863.05	95.28	2007.56

Note: A10 is not included here due to its higher magnesium oxide content, which results in significant differences in batch design compared to other glasses, leading to a loss of comparability.

on a one-dimensional steady state model[29]:

$$\dot{q} = \frac{\vartheta_h - \vartheta_k}{\frac{1}{\alpha_h} + \frac{1}{\alpha_k} + \frac{s_1}{\lambda_1} + \frac{s_2}{\lambda_2} + \cdots + \frac{s_n}{\lambda_n}}$$

where the $\dot{q}$ is the heat flow; ϑ_h and ϑ_k are hot and cold face temperature. α_h and α_k are the heat transfer coefficients of the hot and cold surfaces respectively and s is thickness and λ the thermal conductivity of each layer.

Since the melting temperature of glasses G10 and G08 are 1424°C and 1458°C respectively, the temperature at the crown was assumed to be 1516°C and 1550°C accordingly based on the typical furnace operating temperature of 1550°C above the glass bath.[1] The temperature of the outside crown was estimated to be 154°C.[39] As the crown structure and dimension and refractory does not appreciably change, this provides:

$$\frac{\dot{q}_{G10}}{\dot{q}_{G08}} = \frac{1516°C - 154°C}{1550°C - 154°C} = 97.5\%$$

which roughly indicates that 2.5% of heat loss from the furnace crown can be saved by a 34°C temperature reduction in the crown temperature which corresponds to approxi-

mately a 30°C reduction in the temperature corresponding to log (η/dPa/s) = 2.

6 | CONCLUSIONS

The melting enthalpy of the surveyed commercial glasses and the theoretical energy requirement (TER) of their glass batches were calculated based on assumptions. Melting temperature and glass heat capacity, especially the former, collectively have an impact on the melting enthalpy of glass. The melting enthalpy of glass compositions generally increases linearly with the rise in melting temperature. This result offers insights for the future development of new industrial glass compositions. Based on the current investigation, there is no significant correlation between the theoretical energy requirement (TER) of the designed batch compositions and the melting temperature of the glass. This finding indicates that, under the current conditions, the TER calculated in this study is influenced by multiple factors rather than being solely determined by one factor. However, in the future, with the increase in the amount of added cullet and the development of alternative carbonate-free batch ingredients, the impact of the glass melting temperature on TER will become more pronounced. It is also important to note that the TER calculation used here does not consider the furnace surface heat dissipation, and the reduction in melting temperature will undoubtedly have a positive effect on it.

The calculations also show that a reduction of approximately 30°C in the glass melting temperature (the temperature corresponding to log (η/dPa/s) = 2) can save approximately 2.5% of heat dissipation loss from the furnace crown.

ACKNOWLEDGMENTS

The authors express gratitude for the financial support received from UKRI/EPSRC (TransFIRe Hub, EP/V054627/1). The authors also extend their appreciation to Dr. Nick Kirk and Mr. Adam Frith from Glass Technology Services Ltd. for valuable discussions and technical assistance. For the purpose of open access, the authors have applied a Creative Commons Attribution (CC BY) license to any Author Accepted Manuscript version arising from this submission.

ORCID

Erhan Kilinc https://orcid.org/0000-0002-5280-0275
Paul A. Bingham https://orcid.org/0000-0001-6017-0798

REFERENCES

1. Wallenberger FT, Bingham PA. Fiberglass and glass technology: energy-friendly compositions and applications. New York: Springer; 2009.
2. Butler H J, Hooper PD. Glass waste. In: Letcher TM, Vallero DA, editors. Waste. 2nd ed. Cambridge: Academic Press; 2019. p. 307–22.
3. Global CO_2 emissions in 2019 – Analysis. IEA. 2019. Available from: https://www.iea.org/articles/global-co2-emissions-in-2019. Accessed 31 Dec 2023.
4. Glass sector net zero strategy 2050. British Glass Manufacturers' Confederation. 2023. Available from: https://www.britglass.org.uk/knowledge-base/resources-and-publications/glass-sector-net-zero-strategy-2050. Accessed 31 Dec 2023.
5. Deng W, Backhouse DJ, Kabir Kazi F, Janani R, Holcroft C, Magallanes M, et al. Alternative raw material research for decarbonization of UK glass manufacture. Int J Appl Glass Sci. 2019;14:341–65.
6. UK Department for Business, Innovation & Skills and Department of Energy & Climate Change, Industrial Decarbonisation & Energy Efficiency Roadmaps to 2050: Cross Sector Summary. 2015. Available from: https://www.gov.uk/government/publications/industrial-decarbonisation-and-energy-efficiency-roadmaps-to-2050. Accessed 31 Dec 2023.
7. Glass Futures and its members to continue leading the decarbonisation of energy intensive industries thanks to £18 m of government funding. Glass Futures. Available from: https://www.glass-futures.org/article/?p=mNFl8CFAlrNkhIAfDqgEatzLa1dKERBbhB7dwnjueIThkp9L65e5ebP. Accessed 31 Dec 2023.
8. Glass Futures partners with C-Capture on project awarded £1.7 m in BEIS funding to demonstrate feasibility of next generation, low-cost carbon capture solutions in hard-to-decarbonise industries. Glass Futures. Available from: https://www.glassfutures.org/article/?p=G5A65GmsMpwCqRInsJgiDNINbp0slnebzdvF6tu6gREiFNgbd11diPx. Accessed 31 Dec 2023.
9. Deng W, Spathi C, Coulbeck T, Erhan K, Backhouse D, Marshall M, et al. Exploratory research in alternative raw material sources and reformulation for industrial soda-lime-silica glass batches. Int J Appl Glass Sci. 2020;11:340–56.
10. Deng W, Backhouse D, Kabir F, Janani R, Bigharaz M, Wardlow A, et al. An ancient technology could help deliver decarbonization. Glass Int. 2019;42:47–9.
11. Deng W, Wright R, Boden-Hook C, Bingham PA. Melting behavior of waste glass cullet briquettes in soda-lime-silica container glass batch. Int J Appl Glass Sci. 2019;10:125–37.
12. Deng W, Wright R, Boden-Hook C, Bingham PA. Briquetting of waste glass cullet fine particles for energy-saving glass manufacture. Glass Technol: Eur J Glass Sci Technol A. 2018;59:81–91.
13. Backhouse D, Guilbot A, Scrimshire A, Eales J, Wei D, Bell A, et al. Biomass ashes as potential raw materials for mineral wool manufacture: initial studies of glass structure and chemistry. Glass Technol: Eur J Glass Sci Technol A. 2022;63:19–32.
14. Backhouse D, Wei D, Bingham PA. Biomass ash raw materials investigated for low-carbon glassmaking. Glass Worldwide. 2019;86:74–6.
15. Janani R, Deng W, Backhouse DJ, Kabir-Kazi F, Wieaddo G, Jones AH, et al. Paving the way to net zero by repurposing waste. Glass Int. 2022;45:39–43.

16. Punt Marks Guide. Bucher Emhart Glass. Available from: https://emhartglass.com/node/155. Accessed 5 Dec 2023.
17. Sato Y, Watazumi T, Saeki K. A new method of cutting glass plate, using thermal stress. J Mech Sci Technol. 1977;1:169–82.
18. Bell AMT, Backhouse D, Deng W, Eales JD, Kilinc E, Love K, et al. X-ray Fluorescence analysis of feldspars and silicate glass: effects of melting time on fused bead consistency and volatilisation. Minerals. 2020;10:442.
19. Green Soda-lime-silica container glass SGT11. The Society of Glass Technology. Available from: https://cdn.ymaws.com/sgt.org/resource/resmgr/certificatesofanalysis/green_certificate__11.pdf. Accessed 5 Dec 2023.
20. Hrma PR, Vienna JD, Mika M, Crum JV, Piepel GF. Liquidus Temperature Data for DWPF Glass. Richland, WA (United States): Pacific Northwest National Lab. (PNNL); 1998.
21. American Society for Testing and Materials. Standard practices for measurement of liquidus temperature of glass by the gradient furnace method. Annual Book of ASTM Standards, C 829–81. Gaithersburg: American Society for Testing and Materials; 1990.
22. Lakatos T, Johansson LG, Simmingskold B. viscosity temperature relations in the glass system SiO_2-Al_2O_3-Na_2O-K_2O-CaO-MgO in the composition range of technical glasses. Glass Technol. 1972;13:88–95.
23. Fluegel A. Glass viscosity calculation based on a global statistical modeling approach. Glass Technol-Part A. 2007;48:13–30.
24. Lyle AK. Design and development of glasses for manufacture of containers. Glass Industry. 1961;42:252.
25. Zhernovaya NF, Onishchuk VI, Kurnikov VA, Zhernovoi FE. Rapid evaluation of the workability of container glass. Glass Ceram. 2001;58:329–31.
26. Fluegel A. Global model for calculating room-temperature glass density from the composition. J Am Ceram Soc. 2007;90:2622–5.
27. Fluegel A. Modeling of glass liquidus temperatures using disconnected peak functions. Rochester, NY: Glass and Optical Materials Division Meeting; 2007.
28. Trier W. Glass Furnaces: Design Construction and Operation. Sheffield: Society of Glass Technology; 1987.
29. Sardeshpande V, Gaitonde UN, Banerjee R. Model based energy benchmarking for glass furnace. Energy Convers Manag. 2007;48:2718–38.
30. Bingham P, Marshall M. Reformulation of container glasses for environmental benefit through lower melting temperatures. Glass Technol. 2005;46:11–9.
31. The study on the rational use of energy in The Republic of Bulgaria (II) Chapter 8. GLASS - 8.1 Characteristics of Use of Energy. Tokyo: Japan International Cooperation Agency: Energy Conservation Center; 1994.
32. Madivate C. Calculation of the theoretical energy requirement for melting technical silicate glasses. J Am Ceram Soc. 1998;1:3300–6.
33. Kim DS, Matyáš J. Batch Reactions of a Soda-Lime Silicate Glass (Report for G Plus Project for Libbey Inc.). Richland, WA: Pacific Northwest National Laboratory; 2002. p. PNNL–13994,15001103.
34. Madivate C, Müller F, Wilsmann W. Thermochemistry of the glass melting process—energy requirement in melting soda-lime-silica glasses from cullet-containing batches. Glastech Ber Glass Sci Technol. 1996;69:167–78.
35. Richet P. Heat capacity of silicate glasses. Chem Geol. 1987;62:111–24.
36. Stebbins JF, Carmichael ISE, Moret LK. Heat capacities and entropies of silicate liquids and glasses. Contrib Mineral Petrol. 1984;86:131–48.
37. Pilkington NSG Group. Glass Technology/Raw materials. Available from: https://www.pilkington.com/en/global/knowledge-base/glass-technology/the-float-process/raw-materials. Accessed 15 Mar 2024.
38. Kovačec M, Pilipović A, Štefanić N. Impact of glass cullet on the consumption of energy and environment in the production of glass packaging material. Montreux, Switzerland: Recent Researches in Chemistry, Biology, Environment & Culture; 2011.
39. Efficient crown insulation. Glass Worldwide. 2016;69:123.

SUPPORTING INFORMATION

Additional supporting information can be found online in the Supporting Information section at the end of this article.

How to cite this article: Deng W, Wakelin E, Kilinc E, Bingham PA. A survey of commercial soda–lime–silica glass compositions: Trends and opportunities. I—Compositions, properties and theoretical energy requirements. Int J Appl Glass Sci. 2024;1–14. https://doi.org/10.1111/ijag.16691